The Effect of Maleated Polylactic Acid (PLA) as an Interfacial Modifier in PLA-Talc Composites

Alison C. Fowlks, Ramani Narayan

Department of Chemical Engineering and Materials Science, Michigan State University, East Lansing, MI 48823

Received 15 July 2009; accepted 6 March 2010
DOI 10.1002/app.32380
Published online 30 June 2010 in Wiley InterScience (www.interscience.wiley.com).

ABSTRACT: Polylactic acid (PLA)-talc composites were reactively compatibilized using maleic anhydride-functionalized PLA (MAPLA) as an interfacial additive. The effect of MAPLA was investigated based on evaluation of composite properties and examination of the microstructure using scanning electron microscopy. The incorporation of MAPLA contributed to an increase in the crystallinity of PLA in the composites, and when added in an optimal concentration, showed improved tensile strength. Thermo–mechanical measurements indicated the reinforcement effect of the talc and the coupling effect of the MAPLA inclusion. Microscopic studies revealed the composite microstructures along with the corresponding modes of failure which were in accordance with the mechanical behavior. Overall, this investigation provided experimental evidence of enhanced adhesion at the interface, which is believed to be due to the MAPLA addition. © 2010 Wiley Periodicals, Inc. J Appl Polym Sci 118: 2810–2820, 2010

Key words: biodegradable; reactive extrusion; compatibilization

INTRODUCTION

Increased awareness of major environmental issues has recently spurred great interest in the sustainable management of carbon resources and the development of a safe and effective disposal system for polymeric materials. This has placed demands on the plastics industry to develop cost-effective, sustainable alternatives to conventional petroleum-based plastics, with specific emphasis on the development of biobased materials for use in short life, disposable applications. Polylactic acid (PLA) is a biodegradable, aliphatic polyester derived from renewable resources and has recently been placed at the forefront of research objectives to meet this very need. Its transparency, high strength, and stiffness make it superior to many other biobased polymers currently available on the market. However, its shortcomings are what prevent its large-scale competition with petroleum-based polymers. For this reason, PLA-based materials are increasingly being studied in an effort to improve its properties and to gain commercial acceptance with more widespread utility.

PLA-matrix composites are becoming progressively important, providing the advantage that one can, in principle, tailor properties to be suitable for specific applications with the addition of fillers. Whether they are organic or inorganic in nature, fillers can be either fibrous or particulate, both of which have been incorporated into PLA with the goal of increasing its performance capabilities. For instance, to increase the thermal resistance of PLA, researchers have incorporated into it clay,[1,2] carbon fibers,[3] and glass fibers,[4] each with the aim of increasing crystallization. Urayama et al.[5] studied the effects of particle-type and whisker-type fillers on the thermal and mechanical properties of PLA. In their study, the fillers of interest were calcium silicate, potassium titanate, and aluminum borate. The resultant thermal properties indicated that there was no significant effect of the fillers on the glass transition and melting temperatures. However, the composites did show faster crystallization as compared with the neat polymer. Mechanical data showed that, overall, the whisker-type filler was more effective than the particle-type with respect to matrix reinforcement, with the highest tensile strength being associated with the potassium titanate and aluminum borate whiskers. Izod impact tests of the composites showed only a slight improvement over the control specimens.

Other inert fillers, such as talc and calcium carbonate, have also made their way into PLA-matrix composites for the above reasons, as well as to reduce cost and improve mechanical properties. Thakur et al.[6] found that talc acted as a nucleating agent in PLA and increased the number of spherulites during crystallization. Kolstad[7] confirmed this finding

Correspondence to: A. C. Fowlks (fowlksal@msu.edu).

and concluded that 6% of talc gave a 500-fold increase in nucleation density. Recently, Hiljanen-Vainio et al.[8] enhanced the mechanical properties of a lactic acid based poly(ester-urethane) via the addition of both organic and inorganic fillers. Huda et al.[9] incorporated talc into PLA in a simple blend and reported a decrease in tensile strength, but a with 92% increase in tensile modulus. In that same study, the heat distortion temperature was reported to have increased by 24°C.

Although, a number of researchers have produced PLA-based composites, the most important issue still must be addressed: the compatibility between the matrix and the filler. Based on a review of the published literature, it is apparent that a simple uncompatibilized mixture of PLA and filler (regardless of filler type) is insufficient for producing composites with good end properties. In fact, in some cases, simple admixing may deteriorate the existing properties of the matrix material as any addition can disrupt the homogeneity of the material and act as a stress concentration point. Further, the nonpolar nature of PLA makes it difficult to react with reinforcements containing polar moieties such as natural fibers, talc and starch, resulting in poor dispersion, a lack of sufficient adhesion and a reduction in properties. This presents a major disadvantage to PLA matrix composites, providing that they are unable to reach their full performance potential. Consequently, the use of coupling agents or compatibilizers is essential to promote chemical bonding across the filler-matrix interface.

Substantial experimental efforts have been made in an attempt to improve the phase interaction of PLA-based composites by reactive compatibilization. This is typically done by modifying either one or both of the composite constituents by grafting or by the incorporation of a third component (a coupling agent) that acts to reduce the interfacial tension between the phases and improves the dispersion of the filler within the PLA matrix. One commonly used coupling agent is maleic anhydride (MA), a polar monomer that has been extensively studied and shown to be quite effective in improving the adhesion between two or more phases due to its highly reactive nature.[10–13] The dual reactivity of MA stems from the free radical reactivity of the double bond and the functional reactivity of the cyclic anhydride. Once grafted, an MA-based copolymer can preferentially reside at the interface and act as a bridge between binary phases to improve interfacial adhesion, and thereby result in a finer dispersion and more stable morphology.

Although MA has long been grafted onto polyolefins, only recently has it been grafted onto biodegradable polyesters,[14–17] particularly PLA. Carlson et al.[18,19] pioneered the development of maleated PLA (MAPLA) and reported considerable improvement in adhesion in starch filled composites on the basis of morphology. Those results have been confirmed by reported improvements in mechanical behavior and by investigation of microstructural and interphase thickness.[20] Some authors have shown that, despite inducing physical improvements of the composite, the use of MAPLA as a matrix leads to degradation of the overall material. Therefore, to minimize degradation and maintain the molecular integrity of the PLA matrix, MAPLA has been used as an interfacial agent in various composite systems. Plackett,[21] for example, studied the use of MAPLA in PLA-matrix composites filled separately with wood fiber, nanoclay, and jute fiber mat. He reported enhanced adhesion in the PLA/wood fiber system, but no improvement was seen in the latter two. Others[22] have produced PLA-based composites filled with cellulose powder, corn starch, and wood flour that were compatibilized with MAPLA and reported improvements in both tensile behavior and morphology. Petersson et al.[23] reported improved phase interaction and mechanical properties by the use of MAPLA as a compatibilizer in layered-silicate nanocomposites.

Based on the literature, the use of MAPLA is an effective method to compatibilize PLA-based composites compounded with various fillers, but no studies have been performed related to its coupling effect in talc-filled systems. In this work, talc was selected as a low-cost filler. Its structure is a trioctahedral phyllosilicate with the simplified molecular formula, $Mg_3Si_4O_{10}(OH)_2$. Talc comprises of a majority hydrophobic face; however, its edge surface is composed of ~10% hydroxyl groups, which are available for reacting with hydrophilic moieties, such as MA to form covalent bonds.[24] Thus, this project aims at investigating the effect of a MA functionalized PLA (containing 0.7% MA) as an interfacial modifier in PLA-talc composites. The amount of MAPLA was varied between 3 and 10% and the composites were studied on the basis of mechanical, thermal and morphological properties.

MATERIALS AND METHODS

PLA (Nature Works 3051D) was obtained from Cargill Dow (Minneapolis, MN). It had a weight-average molecular weight, M_w of ~ 140,000 g/mol, a density of 1.24 g/cm^3, a glass transition temperature, T_g of 54°C and a melting temperature, T_m of 153°C. Talc (Artic Mist) was supplied by Luzenac America, having a median diameter of 2 μm. Before extruding, the PLA and talc were separately dried for 24 h at 80°C to remove excess moisture. MA was purchased from Sigma-Aldrich Chemical Company and 3,6,9-Triethyl-3,6,9-trimethyl-1,4,7-triperoxonane (T301)

TABLE I
Injection Molding Temperatures for PLA and PLA/Talc Composites

Sample composition	Temperature (°C)				
	Zone 1	Zone 2	Zone 3	Nozzle	Mold
PLA	210	202	199	196	24
MAPLA	182	177	177	171	24
PLA-Talc-(MAPLA) composites	212	210	210	205	24

was supplied by Akzo Nobel. Both were used as received.

MA grafting

MA was grafted onto the PLA backbone according to a modified experimental protocol developed by Carlson et al.[18] Dried PLA pellets were combined with 0.5% T301 and 2% MA and manually tumble-mixed before being introduced into a Century ZSK-30 twin-screw corotating extruder using a mechanical feeder set at a rate of 150 rpm. The barrel of the extruder was divided into ten temperature zones, corresponding to the following temperature profile: 25/90/165/180/180/180/180/180/175/170. The screw speed was maintained at 100 rpm and a continuous flow of nitrogen was purged throughout the extruder. Unreacted MA and excess moisture were removed by applying vacuum at the vent port. The extrudate was cooled in a water bath and pelletized downstream. The pellets were collected and dried for 24 h before further processing. The grafting yield was determined by titrimetric analysis according to a slight modification of a procedure presented by Li et al.[25] and calculated to be 0.7% ± 0.0% MA.

Compounding PLA/talc composites

PLA/talc composites were compounded by extrusion using a Century ZSK-30 twin-screw corotating extruder. PLA pellets were manually premixed with 40 wt % talc and varying amounts of MAPLA. The MAPLA was incorporated by replacing 3, 5, and 10% of the PLA matrix. After mixing, the components were fed into the extruder at 150 rpm and extruded with a screw speed of 100 rpm under the following temperature profile: 25/95/145/165/175/180/180/180/175/170. The extruded strand was collected, pelletized and dried at 80°C for 24 h before further processing.

Injection molding

The dried extruded pellets were injection molded into tensile bars using a Cincinnati Milacron VSX85 model equipped with an ASTM Type IV mold (16.51 cm × 1.19 cm × 0.32 cm). The processing conditions for injection molding are shown in Table I.

CHARACTERIZATION

Differential scanning calorimetry

The melting and crystallization behavior of the composites were investigated using differential scanning calorimetry (DSC). The samples were heated to 200°C at 20°C/min and held for 5 min to erase the thermal history. The samples were then cooled to −30°C at a cooling rate of 3°C/min to observe crystallization behavior, then reheated to 220°C at 3°C/min. Crystallization and melting temperatures were obtained from the cooling and second heating scans, respectively.

The crystallinities of the composites were calculated according to the following equation:

$$X_c = \frac{\Delta H_m}{\Delta H_m^0 \times \phi_{\mathrm{PLA}}} \times 100\%$$

ΔH_m and ΔH_m° are the respective enthalpies of fusion (in J/g) of the composites and of a PLA crystal of infinite size, whose reported value is 93.7 J/g. Φ_{PLA} is the weight fraction of PLA in the composite.

Mechanical properties

A United Testing System (UTS) Mechanical Testing Equipment (Model SFM-20) fitted with a 1000 lb load cell was used to determine tensile properties of the samples. Before testing, the tensile bars were conditioned at 25°C and 50% relative humidity for at least 40 h per the ASTM D638 standard. The crosshead speed was set at 0.5 in/min. At least five specimens were tested and the average values were reported.

Thermo-mechanical properties

Dynamic mechanical measurements were performed to investigate the storage modulus, loss modulus and tan delta values as a function of temperature for the compatibilized PLA/talc composites. Measurements were run on rectangular bars with dimensions of 57.0

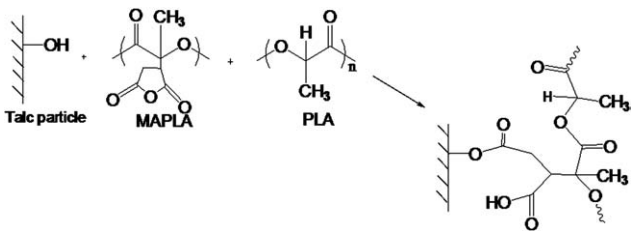

Figure 1 Proposed reaction between PLA, talc, and MAPLA yielding a monoester on the surface of the talc particle.

mm × 3.0 mm × 12.7 mm using a TA 2980 DMA equipped with a dual-cantilever bending clamp at a frequency of 1 Hz and a heating rate of 10°C/min over a temperature range of 24°C to 140°C. All measurements were performed and properties were reported in accordance with ASTM D 4065.

Scanning electron microscopy

Examination of the composite microstructure was carried out using two separate scanning electron microscopy (SEM) techniques. For the first set, injection molded specimens were cut into 2.5-cm long rectangular sections. They were then mounted in epoxy, and polished. Each sample was coated with osmium and imaged using the backscattered electron imaging mode at an accelerating voltage of 12 kV and a working distance of 15 mm. The second technique was performed on the tensile fracture surfaces. The samples were dried overnight to remove any sorbed water before being mounted onto an aluminum stub and sputter-coated with a thin layer (21 nm) of gold. Micrographs were imaged using secondary electrons at an accelerating voltage of 15 kV and a working distance of 15 mm.

Statistical analysis

Statistical analysis was performed using *SPSS* for Windows. Data were compared by one-way analysis of variance (ANOVA) and a Tukey post-ANOVA test. The mean values were considered significant at the 0.05 level ($P \leq 0.05$).

RESULTS AND DISCUSSION

Proposed reaction mechanism

It was expected that maleated PLA would react with talc via an esterification reaction. In Figure 1, the proposed reaction is shown to occur between the anhydride group on the functionalized PLA and the hydroxyl groups on the edge surface of the talc particle, resulting in the formation of a monoester on the surface of the talc particle. This compatibilization would result in effective stress transfer across the interface and allow the composite to withstand higher stresses upon loading.

The molecular weight of a polymer is known to significantly affect its surface tension. In general, surface tension decreases as molecular weight decreases.[26] Presumably, the lower molecular weight of MAPLA would enable good wetting during processing, allowing MAPLA polymers/oligomers to coalesce at the interface of the PLA and talc, creating an interphase. This thin region is believed to be responsible for stronger interaction between the phases, as evidenced by the improvements in properties that will be discussed in the subsequent sections.

DIFFERENTIAL SCANNING CALORIMETRY

Table II summarizes the impact that the addition of talc and the MAPLA has on the glass transition, melting, and crystallization temperatures, an on the crystallinity of PLA. The talc, alone increased the crystallinity of the PLA component from 16% to nearly 26%. This increase in crystalline fraction is in agreement with the well known nucleating effect of mineral particles in semicrystalline materials.[27,28] An important step in investigating the efficacy of an interfacial modification induced by a coupling agent is to examine the effect that it has on the glass transition temperature. The incorporation of MAPLA into the composite resulted in no significant changes in the T_g nor did it have any major effect on melting temperatures (Fig. 2). However, the addition of both talc and MAPLA did show enhanced crystallinity of PLA ($P = 0.05$) when compared to the unfilled

TABLE II
Melting, Crystallization, and Glass Transition Temperatures for PLA/Talc Composites

Sample composition	T_g (°C)	T_c (°C)	$T_{m,1}$ (°C)	$T_{m,2}$ (°C)	χ (%)
PLA	58.1 ± 1.0[a]	106.9 ± 3.1[a]	146.5 ± 1.5[a]	153.7 ± 1.2[a]	16.1 ± 1.1[a]
MAPLA	55.7 ± 0.4[b]	115.6 ± 2.6[b]	144.9 ± 1.9[a]	154.1 ± 0.9[b]	25.7 ± 2.0[b]
PLA/Talc (60:40)	56.7 ± 0.7[ab]	107.4 ± 0.8[a]	147.7 ± 0.7[a]	154.6 ± 0.9[b]	25.5 ± 1.1[b]
PLA/MAPLA/ Talc (57:3:40)	56.3 ± 0.3[ab]	109.6 ± 0.6[a]	147.0 ± 0.2[a]	153.8 ± 1.6[b]	27.3 ± 1.0[b]
PLA/MAPLA/ Talc (55:5:40)	54.6 ± 0.6[b]	107.4 ± 1.0[a]	147.8 ± 0.9[a]	154.7 ± 0.4[b]	30.0 ± 0.6[c]
PLA/MAPLA/ Talc (50:10:40)	53.6 ± 0.5[b]	109.9 ± 1.5[a]	148.0 ± 1.3[a]	154.9 ± 0.5[b]	32.9 ± 0.2[d]

[a–d]Letters within the same column represent statistical significant differences at the 95% confidence level.

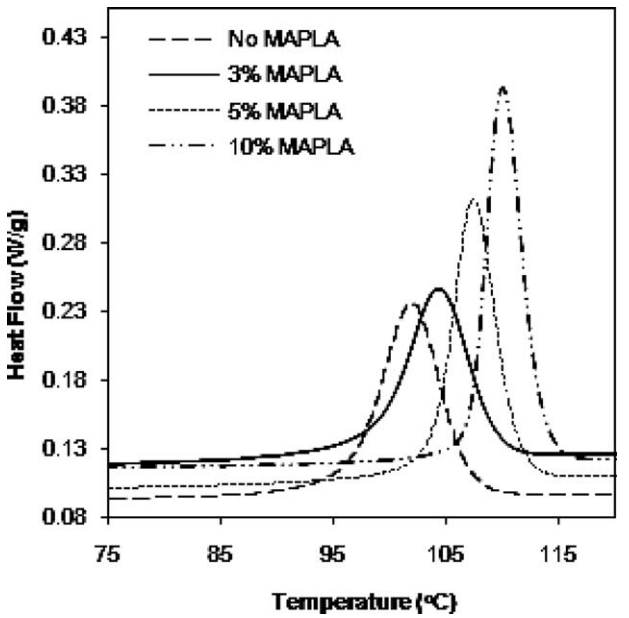

Figure 2 DSC thermograms of PLA/talc composites revealing the effect of MAPLA on the melting behavior.

polymer. In the composites the higher crystallization temperatures (measured upon cooling) suggests the ability of the polymer to crystallize sooner and to a greater extent as shown in Figure 3. According to Feng,[29] to fully understand the effect of a maleated coupling agent on the melting and crystallization behavior of a composite, two factors must be considered. The first is that, MAPLA is of lower molecular weight (based on previous GPC data not shown) and, because of this, may have a lubricating effect on the PLA matrix. The second consideration is of the expected covalent and acid-base interactions induced between the anhydride on the MAPLA and the hydroxyl groups on the talc. Good interaction between the two functional groups could possibly restrict the mobility of the molecules, thus, the grafted MAPLA could disrupt the regularity of the PLA chain and hinder crystallization. Alternatively, the low molecular weight of MAPLA could promote chain movement of the shorter chains and favor crystallization. In this case, the latter is believed to have occurred. The crystalline fraction increased progressively with the level of MAPLA. The MAPLA contributed to more freely moving polymer chains and the enhanced chain mobility permitting higher molecular orientation and better filler dispersion, which in turn led to increased crystallization activity.[30]

Mechanical properties

As was evidenced by the increase in crystallinity of the PLA component, the incorporation of talc influences gradual structural changes in the system. In this way, the interactivity between composite components, combined with the addition of MAPLA and factors such as orientation and dispersion of talc, can affect the properties of the composites. Thus, the mechanical behavior of the composites was investigated to study the extent of interaction between PLA and talc with varying amounts of MAPLA. The effects of the interfacial phenomena on various parameters, namely, the tensile strength, elongation at break, and Young's modulus are presented in Table III.

Generally, the incorporation of fillers into a matrix may increase or decrease the tensile strength of the resulting composite, depending on the filler shape. Particulate fillers, such as talc tend to decrease the strength of the composites due to their lower ability to support stresses transferred from the polymer matrix. Interestingly, in this case, the sole addition of talc had no significant effect on the tensile strength. Adding MAPLA, however, increased the tensile strength, from 60 MPa for the unmodified composite, to 66 MPa at 3% MAPLA up to 72 MPa at 5% MAPLA, at which the tensile strength reached a maximum; beyond which it dramatically dropped to 24 MPa. From this, it may be inferred that increasing the amount of anhydride groups in the system increases the number of the acid-base interactions and the degree of hydrogen bonding, which leads to a stronger interaction between the filler and the matrix. With excess amounts of anhydride groups, however, the coupling effects of MAPLA could have been counteracted by hydrolysis of the bulk polymer caused by the increased amount of end groups

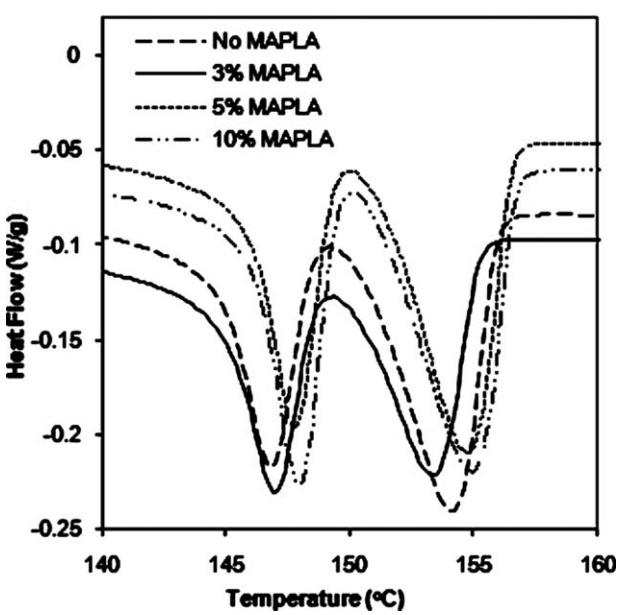

Figure 3 DSC thermograms of PLA/talc composites revealing the effect of MAPLA on the crystallization temperature.

TABLE III
Tensile Properties of PLA/Talc Composites

Sample	Tensile strength (MPa)	Young's modulus (GPa)	Elongation at break (%)
PLA	58.7 ± 2.2[a]	3.6 ± 0.2[a]	4.3 ± 1.0[a]
MAPLA	60.2 ± 2.1[a]	4.0 ± 0.2[a]	3.9 ± 0.8[a]
PLA/Talc (60:40)	59.6 ± 2.2[a]	7.0 ± 0.4[b]	1.1 ± 0.2[b]
PLA/MAPLA/Talc (57:3:40)	66.0 ± 3.1[b]	10.1 ± 0.1[c]	0.9 ± 0.1[b]
PLA/MAPLA/Talc (55:5:40)	72.4 ± 1.8[c]	11.1 ± 1.9[c]	1.5 ± 0.1[b]
PLA/MAPLA/Talc (55:10:40)	24.1 ± 2.3[d]	11.4 ± 1.7[c]	0.3 ± 0.1[c]

[a–d]Letters within the same column represent statistical significant differences at the 95% confidence level.

which may have contributed to the decline in tensile strength.

In all of the composites, the most prominent physical effect of the talc was observed to be the stiffening effect. This is because the Young's modulus of talc (170 GPa)[31] is significantly higher than that of PLA and also because of the enhanced crystallization of the composites. The Young's modulus increased to 10 GPa in the 3% MAPLA samples and remained fairly constant thereafter. This is most likely associated with talc particles being more dispersed throughout the PLA in the samples containing MAPLA and could be an indication of efficient stress transfer from polymer matrix to filler as a result of increased interaction.[9] The higher crystallinity that was seen with the mere addition of talc may have also contributed to the increase in modulus because, in general, the crystalline fraction can affect the extent of intermolecular secondary bonding. Although the crystallinity increased with MAPLA content, the modulus remained constant for all samples containing MAPLA. Therefore, no causal relationship was identified between the crystallinity of the compatibilized composites and the modulus.

Also in Table III are the elongation at break values for the composites. Upon the addition of talc to the inherently brittle PLA, the elongation values dropped from 4% to 1%. Elongation at break is sensitive to the addition particulate fillers that may form areas of stress concentration and initiate cracking. Among the compatibilized composites, no significant changes were seen. Therefore, no correlation could be drawn between elongation and MAPLA concentration.

Moreover, the tensile behavior of the composites suggests that the MAPLA improved the wettability of the filler with the polymer and improved the adhesion at the interface. In addition, the results show that only a small amount of MAPLA is needed to act as an interfacial modifier to enhance the properties, as was seen by the sudden decrease in tensile strength with high MAPLA content. This confirms the existence of a critical amount of MAPLA, which has an ultimate effect on the macroscopic properties of the composite. In this work, the goal of the interfacial agent was to bridge the surfaces of talc and PLA by providing sufficient interfacial adhesion. However, too much interfacial agent was seen to have an adverse reaction, lending to the formation of an interphase that is too thick, limiting interfacial interactions. Therefore, it was postulated that there exists an optimum level of MAPLA that provides the most favorable interactions across the interface of the PLA and talc.[27,32]

THERMO-MECHANICAL PROPERTIES

Dynamic mechanical analysis (DMA) of materials provides a deeper understanding of molecular relaxation mechanisms and their relationship with microstructure. In composites, DMA can be used to characterize the filler-matrix interactions. In this study, dynamic mechanical tests were performed to study the response of the composite to periodic forces. Such experiments enabled the mechanical damping and elastic modulus to be measured simultaneously. By doing so, it was possible to obtain valuable information on the relaxation mechanisms correlated to the microstructure of the composite. The peaks obtained from the loss modulus (E'') and loss factor ($\tan \delta$) can be related to the molecular motion of the polymer. The storage modulus (E') curve provides information on the elastic behavior.

Figure 4 shows representative curves of the storage moduli (E') of PLA and its composites as a function of temperature. Consideration over the entire temperature span shows that all of the specimens followed an identical trend. The curves of the composites and the PLA each showed significant decreases in modulus in the range of 65–75°C. This temperature range correlates to the region where the molecules underwent a transition from being glassy to rubbery and there was minimal contribution of stiffness to the matrix.[33] At temperatures below this transition the incorporation of talc in the PLA matrix

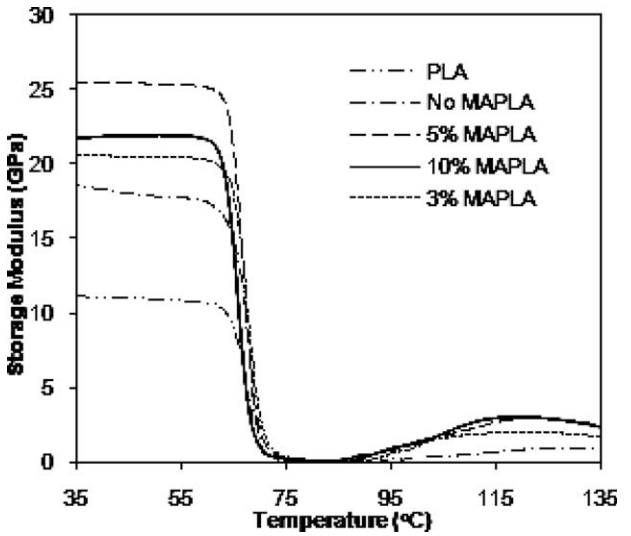

Figure 4 Storage modulus curves of PLA and PLA/talc composites.

increased the elastic component of the system. This was expected since most inorganic fillers, including talc, have moduli at least one order of magnitude higher than most polymers. The increase in E' within the low-temperature region is indicative of the reinforcement effect, which allows effective stress transfer from the PLA matrix to the talc filler, leading to a higher number of PLA-talc interactions and an increase in the load-bearing capabilities.[34] Further investigation of E' at the glass transition temperatures (the respective inflection points of the curves) gives insight into the relationship between the storage modulus and the compatibilization effect. The highest modulus value corresponds to the 5% MAPLA system, followed by 10% MAPLA, 3% MAPLA, 0% MAPLA, and lastly PLA. The increase in storage modulus can be attributed to enhanced interfacial adhesion. The sample containing 10% MAPLA displayed a modulus lower than that of the 5% MAPLA sample. The lower storage modulus may be associated with the increased degradation in this sample (due to hydrolysis) and to the previously mentioned theory of too much interfacial modifier preventing adequate interactions across the composite interface. This is also believed to be the cause for the reduction in tensile strength at this MAPLA composition. Beyond the glass transition region, another plateau region is apparent. This recovery of E' is an effect typical of cold crystallization of the amorphous regions in the polymer, a phenomenon commonly seen in PLA.[35]

Figure 5 shows curves representing the tan δ trends as functions of temperature for PLA and its talc-filled composites. Tan δ is defined as the ratio of the loss modulus to the storage modulus (E''/E'). It is sensitive to the balance of heat dissipated and energy stored and can be used to detect thermochemical relaxations. The tan δ peaks remained at nearly the same temperatures for all of the composites except for that containing 10% MAPLA, which shifted to a lower temperature. This can be attributed to the lower molecular weight of the composite modified with 10% MAPLA. Peak intensities were affected by both the presence of talc and the compatibilization effect. Talc reduced the mobility of the polymer chains, resulting in lower tan δ values. The MAPLA addition also decreased the tan δ values accordingly.

For the compatibilized composites, it is possible to observe a correlation between the intensity of the tan δ peak and the interfacial adhesion. All of the curves displayed a similar tendency until a temperature of about 80°C was reached, at which the 10% MAPLA curve showed a small shoulder. This effect could imply, at 10% of MAPLA, the existence of a third component, rather than an interfacial additive in a two-phase system.[27]

The loss modulus curves, E'', are shown in Figure 6. The temperatures denoting the maxima of the loss modulus curves are representative of the glass transition temperatures due to the motions associated with unrestricted amorphous PLA. From the figure it can be seen that the T_g value for the composite containing 3% MAPLA shifted to a slightly higher temperature, the T_g of the 10% MAPLA system shifted to a lower temperature, while the 5% MAPLA system remained the same as the neat polymer. This suggests that 5% MAPLA may be a more efficient compatibilizer than the other concentrations. It should be noted, however, that the T_gs obtained from DMA are quite different from those obtained

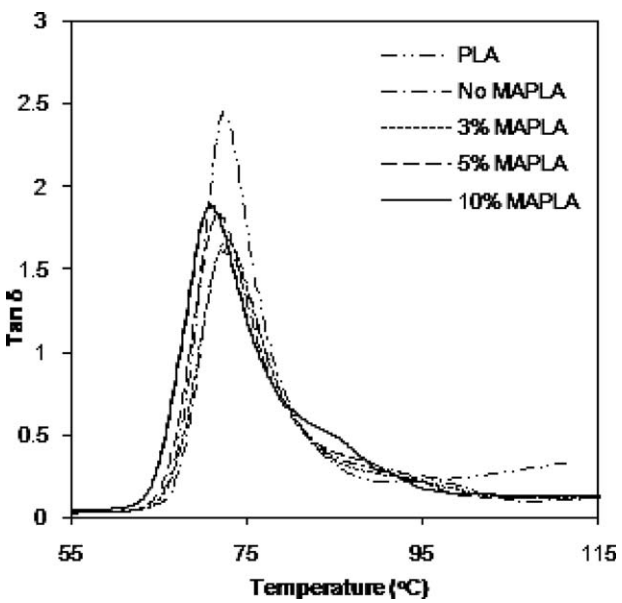

Figure 5 Tan δ curves of PLA and PLA/talc composites.

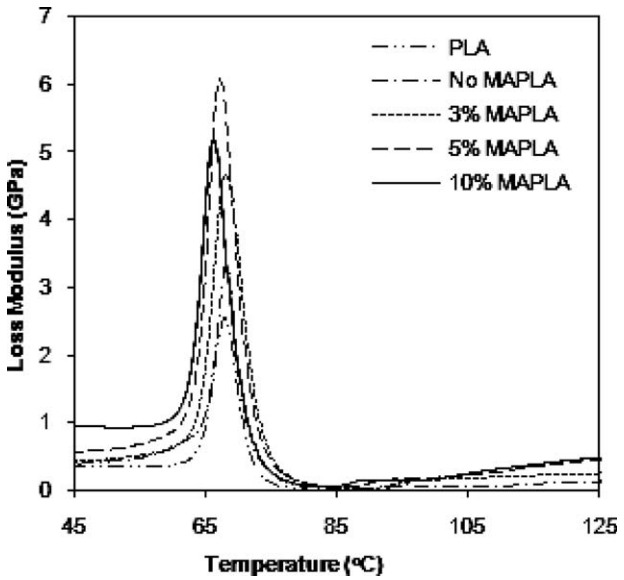

Figure 6 Loss modulus curves of PLA and PLA/talc composites.

from the DSC thermograms and may even show a slight contradiction. This discrepancy can be attributed to a difference in chain mobility as a result of different experimental conditions. The kinetics of the glass transition, the heating rate, and the loading frequency each has some impact on the molecular mobility. Therefore, DMA is a more sensitive tool than DSC in determining the thermal transitions of polymers.[36]

Furthermore, the peak heights of the loss modulus curves are associated with the damping of the material and are related to the energy converted into heat upon deformation. The composites had higher loss moduli than PLA because the presence of talc disrupts the polymer bulk, as the mineral particles are coated by the amorphous phase. The addition of MAPLA at the interface further increased the loss modulus values. The highest peak corresponds to the 5% MAPLA composite, followed by the 10% MAPLA composite, the 3% MAPLA composite, and finally the unmodified composite. Further, a pronounced broadening was seen in the loss moduli of the compatibilized composites, bringing about a transition region with high damping over a temperature range a few times greater than that for the unfilled polymer. The broadening effect as well as the increase in the E'' can be attributed to a combination of the high surface area of the fillers and the strong interaction between PLA and talc. It is possible that the stronger interaction resulted in the partial immobilization of the polymer chains due to adsorption of polymer on the talc surface. The restriction of the polymer chains induced by talc caused a change in density of the packing of the polymer and increased the loss modulus.

Scanning electron microscopy

The morphology and microstructure of composite materials play a significant role in the prediction of macroscopic properties. The PLA-talc composite microstructure was examined using backscattered electrons to effectively observe the size, dispersion, and orientation of the talc particles within the PLA matrix. Unlike secondary electrons, backscattered electrons are primary beam electrons that have been elastically scattered by nuclei and are strongly dependent on the average atomic number of the sample. The backscattered electron images of the polished samples clearly show contrast based on the local chemical composition of the material. Talc, having a higher average atomic number than PLA is revealed as white particles in the micrographs displayed in Figures 7–10. In the sample that contains no MAPLA (Fig. 7), large talc agglomerates are present. The talc particles are relatively unevenly distributed and show no orientation. This configuration is as opposed to those samples containing MAPLA (Figs. 8–10), all of which display talc particles that are more evenly dispersed within the matrix and exhibit axial orientation.

Fracture surface analysis

Postmortem investigation of the PLA-talc composite fracture surfaces provided significant insight into fracture mechanisms and morphological changes that led to the differences in the fracture behavior. The microstructures of the composites were correlated with their fracture surfaces to help elucidate the mode of failure. Each of the composites' topographical micrographs was examined to lend evidence to the assertion of improved interfacial adhesion with added MAPLA. Although all of the

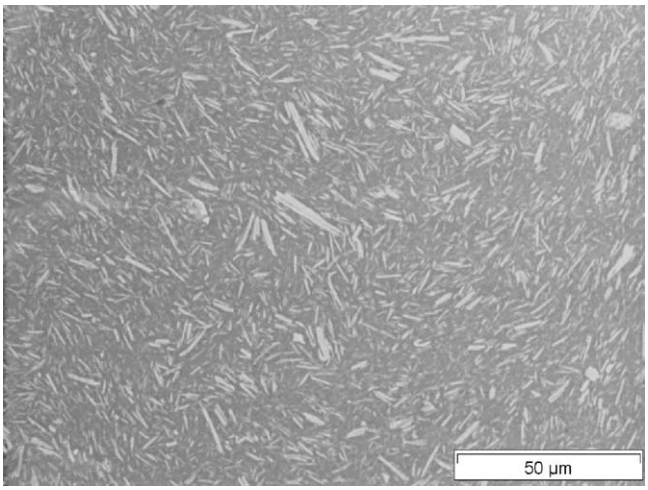

Figure 7 Backscattered electron image of PLA-talc composite containing no MAPLA.

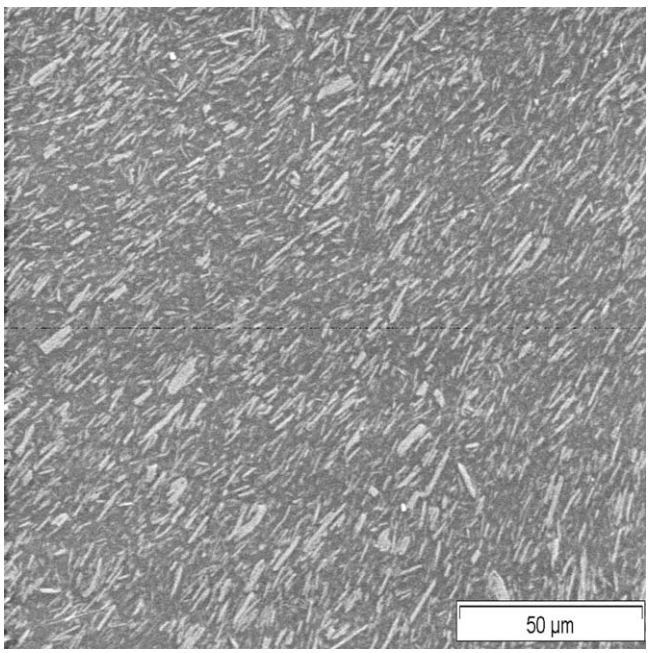

Figure 8 Backscattered electron image of PLA-talc composite containing 3% MAPLA.

composites demonstrated brittle behavior due to the inherently brittle nature of PLA, one of two failure mechanisms was shown to be dominant (1), failure of the PLA matrix or (2) debonding via platelet pull-out.

The micrograph of the composite without added MAPLA displays typical characteristics of an incompatible composite (Fig. 11). In it, a large number of voids appear, resulting from talc platelet debonding. The distinct edges of the talc particles with no polymer adhered to the surface indicate behavior representative of a multicomponent system in which there is little or no adhesion at the interface.

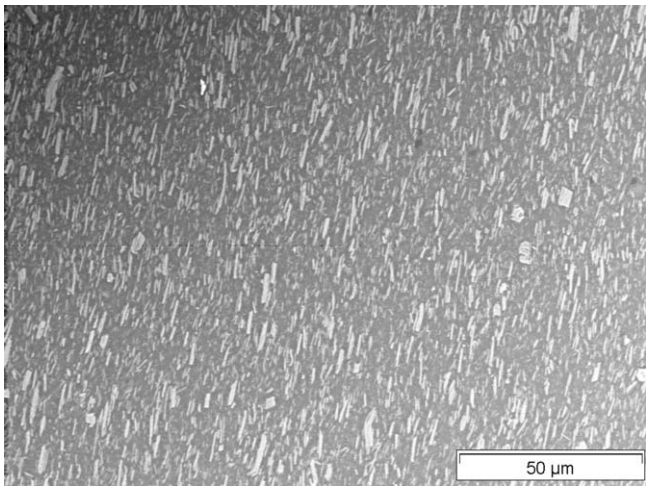

Figure 9 Backscattered electron image of PLA-talc composite containing 5% MAPLA.

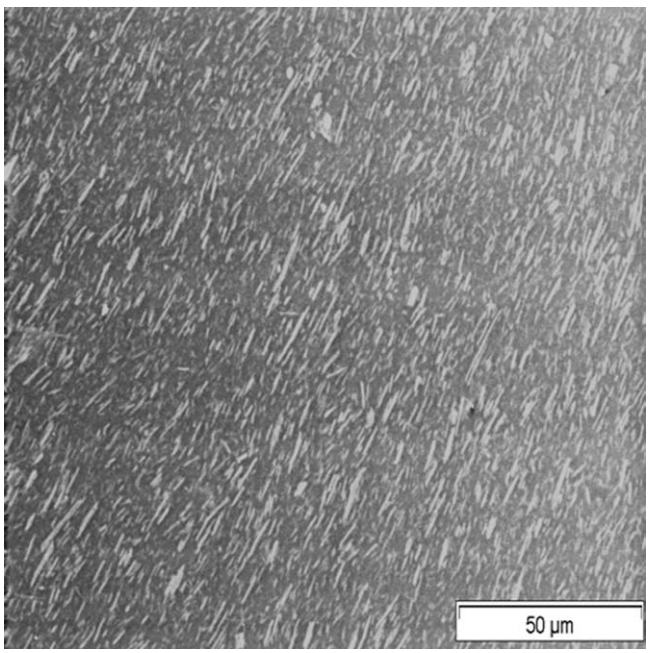

Figure 10 Backscattered electron image of PLA-talc composite containing 10% MAPLA.

In the composite containing 3% MAPLA, shown in Figure 12, it can be seen that many of the talc particles are imbedded within the polymer matrix. Less distinction is seen between talc and PLA. Fewer cavities and edges are present around the talc particles and the talc platelets are coated with PLA, which indicates an increase in adhesion. In addition, the talc platelets are more imbedded within the polymer, which causes the talc particles to appear smaller than in the uncompatibilized composite.

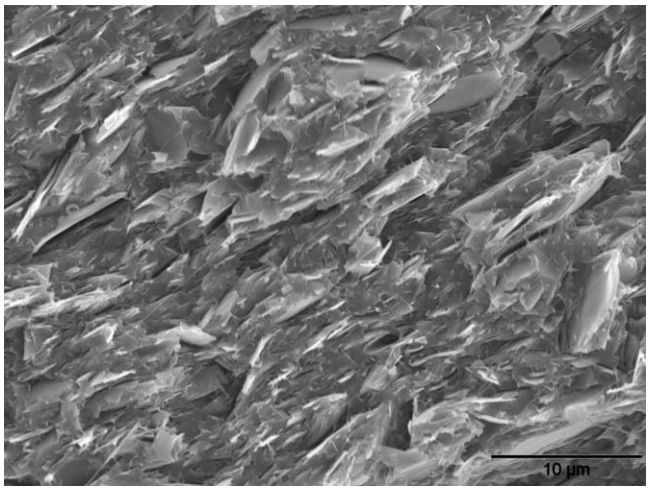

Figure 11 Secondary electron SEM micrograph of PLA-talc composite with no added MAPLA indicating little or no adhesion between talc particles and PLA matrix as evidenced by platelet pull-out.

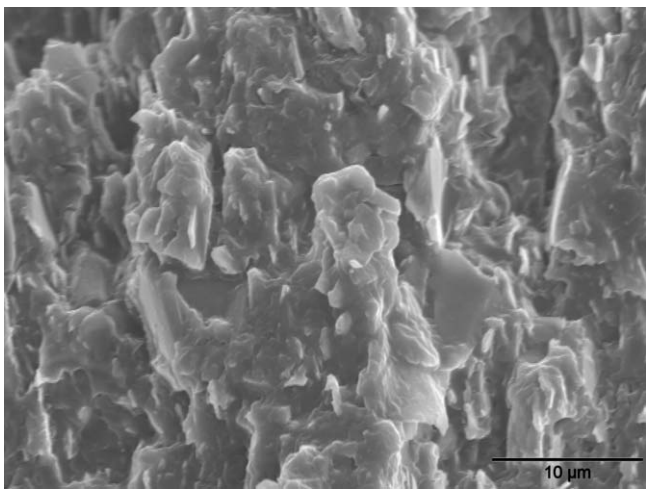

Figure 12 Secondary electron SEM micrograph of PLA-talc composite containing 3% MAPLA denoting slight to moderate adhesion between talc and PLA.

In Figure 13, the fracture surface of the composite with 5% MAPLA shows a very different morphology from the other composites, one that is quite distinctive of a more ductile failure. The morphology of this specimen shows significant localized deformation of the PLA matrix in the form of fibrils. It is also evident that the talc particles are more deeply lodged within the matrix, and that failure occurs within the polymer, as shown by the deformation of the PLA, rather than by debonding at the interface. This suggests better wetting of the talc by the PLA in this system. These observations substantiate the higher mechanical properties that were exhibited in this sample, since stronger adhesion permits an applied load to be effectively transferred from the matrix to filler.

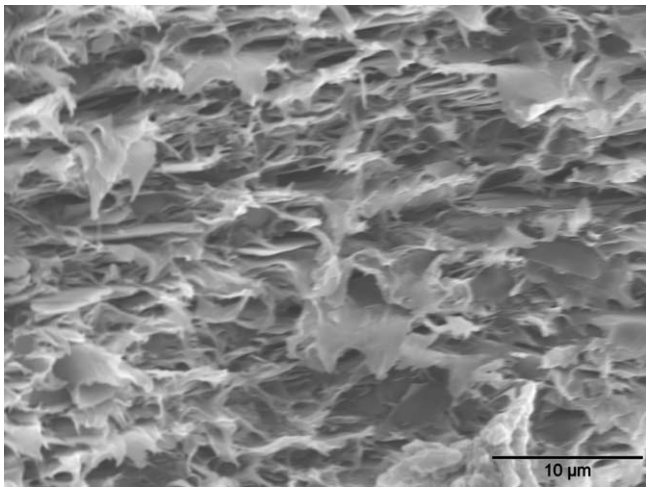

Figure 13 Secondary electron SEM micrograph of PLA-talc composite containing 5% MAPLA revealing enhanced adhesion and a more ductile fracture.

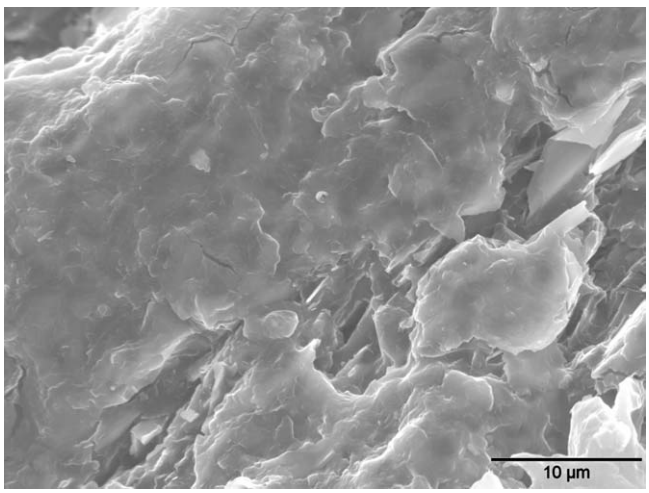

Figure 14 Secondary electron SEM micrograph of PLA-talc composite containing 10% MAPLA displaying a flat surface texture, indicating brittle composite failure in the PLA matrix.

The 10% MAPLA system, in Figure 14, shows behavior characteristic of a brittle material. In materials that undergo brittle fracture, there is rapid crack propagation and very little plastic deformation, yielding a flat surface. It was also interesting that throughout this particular sample composition, two microstructures were apparent: a very flat surface and one in which multiple voids were present. This is likely caused by the high concentration of MAPLA exceeding its solubility limit in PLA, resulting in a heterogeneous microstructure and acting as a detriment to the mechanical behavior. It is necessary to note that it was this composition which displayed the poorest tensile strength and the lowest elongation at break. The brittle behavior exhibited by this composite is most likely due to either excess interfacial adhesion between talc and PLA, preventing safe debonding of the constituent phases; or to increased degradation of the composite due to excess MAPLA which lowered the molecular weight of the polymer. These electron micrographs further confirm the existence of a critical value of MAPLA which is necessary to improve the adhesion in PLA/talc composites.

CONCLUSIONS

A maleic anhydride-grafted PLA was employed as an interfacial modifer in PLA-talc composites. Investigation of the mechanical and morphological properties of the composites provided experimental evidence of increased adhesion at the interface between the PLA matrix and the talc filler. These data indicated the existence of a critical value, beyond which no more improvements occurred, as reflected by a

sudden decrease in tensile strength. Thermomechanical properties confirmed this critical value to be at 5% MAPLA. In spite of the improved interfacial coupling with the maleated PLA addition, the elongation at break remained very low, due to the inherent behavior of PLA and the increased crystallinity of the matrix. The morphology of the composites revealed the modes of failure and the dispersion of the talc particles with the matrix; both of which were in accordance with the mechanical properties analyses.

References

1. Krishnamachari, P.; Zhang, J.; Yan, J.; Shahbazi, A.; Uitenham, L.; Lou, J. In Proceedings of the 2007 National Conference on Environmental Science and Technology; Springer: New York, 2009; p 219.
2. Ogata, N.; Jimenez, G.; Kawai, H.; Ogihara, T. J Polym Sci Part B: Polym Phys 1997, 35, 389.
3. Wan, Y. Z.; Wang, Y. L.; Xu, X. H.; Li, Q. Y. J Appl Polym Sci 2001, 82, 150.
4. Kitano, K. JP Patent 2,005,336,220.
5. Urayama, H.; Ma, C.; Kimura, Y. Macromol Mater Eng 2003, 288, 562.
6. Thakur, K. A. M.; Kean, R. T.; Zupfer, J. M.; Buehler, N. U.; Doscotch, M.; Munson, E. Macromolecules 1996, 29, 8844.
7. Kolstad, J. J Appl Polym Sci 1996, 62, 1079.
8. Hiljanen-Vainio, M.; Heino, M.; Seppälä, J. V. Polymer 1998, 39, 865.
9. Huda, M.; Drzal, L.; Misra, M. Ind Eng Chem Res 2005, 44, 5593.
10. Correa, C. A.; Razzino, C. A.; Hage, E. J Thermoplas Comp Mater 2007, 20, 323.
11. Qiu, W.; Zhang, F.; Endo, T.; Hirotsu, T. Polym Comp 2005, 26, 448.
12. Lai, S.-M.; Yeh, F.-C.; Wang, Y.; Chan, H.-C.; Shen, H.-F. J Appl Polym Sci 2003, 87, 487.
13. Karnani, R.; Krishnan, M.; Narayan, R. Polym Eng Sci 1997, 37, 476.
14. Mani, R.; Bhattacharya, M.; Tang, J. J Polym Sci Part A: Polym Chem 1999, 37, 1693.
15. John, J.; Tang, J.; Yang, Z.; Bhattacharya, M. J Polym Sci Part A: Polym Chem 1997, 35, 1139.
16. Arbelaiz, A.; Fernández, B.; Valea, A.; Mondragon, I. Carbohydr Polym 2006, 64, 224.
17. Maliger, R. B.; Mcglashan, S. A.; Halley, P. J.; Matthew, L. G. Polym Eng Sci 2006, 46, 248.
18. Carlson, D.; Nie, L.; Narayan, R.; Dubois, P. J Appl Polym Sci 1999, 72, 477.
19. Carlson, P.; Nie, L.; Narayan, R. Polym Eng Sci 1998, 38, 311.
20. Dubois, P.; Narayan, R. Macromol Symp 2003, 198, 233.
21. Plackett, D. J Polym Environ 2004, 12, 131.
22. Febrianto, F.; Yoshioka, M.; Nagai, Y.; Tahir, P.; Syafii, W.; Shiraishi, N. JBio Sci 2006, 6, 555.
23. Peterson, L.; Oksman, A.; Mathew, P. J App Polym Sci 2006, 102, 1852.
24. Michot, L. J.; Villieras, F.; Francois, M.; Yvon, J.; Le Dred, R.; Cases, J. M. Langmuir ACS 1994, 10, 3765.
25. Li, H.-M.; Chen, H.-B.; Shen, Z.-G.; Lin, S. Polymer 2002, 43, 5455.
26. Park, H.; Park, C. B.; Tzoganakis, C.; Chen, P. Ind Eng Chem Res 2007, 46, 3849.
27. Garcia-Martinez, J. M.; Laguna, O.; Areso, S.; Collar, E. P. J Appl Polym Sci 2001, 81.
28. Karrad, S.; Lopez Cuesta, J.-M.; Crespy, A. J Matl Sci 1998, 33, 453.
29. Feng, D.; Caulfield, D.; Sanadi, A. Polym Compos 2001, 22, 506.
30. Jang, W. J.; Shin, B. Y.; Lee, T. J.; Narayan, R. J Ind Eng Chem 2007, 13, 457.
31. Martinatti, R.; Ricco, T. J Mater Sci 1994, 29, 442.
32. Sun, X.; Zhang, J.-F. Biomacromol 2004, 5, 1446.
33. Rana, A. K.; Mittra, B. C.; Banerjee, A. N. J App Polym Sci 1999, 71, 531.
34. Shah, J. Vinyl Addit Technol 2005, 11, 160.
35. Nazhat, S. N.; Kellomaki, M.; Tanner, K. E.; Bonfield, W. J Biomed Mater Res 2001, 58, 335.
36. Turi, E., Ed. Thermal Characterization of Polymers, 2nd ed.; Academic Press: San Diego, 1991; Vol. 1.